Emmanuelle Schué | Alexey Kopyshev | Jean-François Lutz | Hans G. Börner

Molecular bottle brushes with positioned selenols: Extending the toolbox of oxidative single polymer chain folding with conformation analysis by atomic force microscopy

Journal article | Version of record

Molecular Bottle Brushes with Positioned Selenols: Extending the Toolbox of Oxidative Single Polymer Chain Folding with Conformation Analysis by Atomic Force Microscopy

Emmanuelle Schué,[1] Alexey Kopyshev,[2] Jean-François Lutz [iD],[3] Hans G. Börner [iD][1]

[1]Laboratory for Organic Synthesis of Functional Systems, Department of Chemistry, Humboldt-Universität zu Berlin, Brook-Taylor-Strasse 2, 12489 Berlin, Germany

[2]Institute of Physics and Astronomy, University of Potsdam, 14476, Potsdam, Germany

[3]Universiteć de Strasbourg, CNRS, Institut Charles Sadron UPR22, 23 rue du Loess, Strasbourg 67034 Cedex 2, France

Correspondence to: H. G. Börner (E-mail: h.boerner@hu-berlin.de)

ABSTRACT: A synthesis route to controlled and dynamic single polymer chain folding is reported. Sequence-controlled macromolecules containing precisely located selenol moieties within a polymer chain are synthesized. Oxidation of selenol functionalities lead to diselenide bridges and induces controlled intramolecular crosslinking to generate single chain collapse. The cyclization process is successfully characterized by SEC as well as by ^{1}H NMR and 2D HSQC NMR spectroscopies. In order to gain insight on the molecular level to reveal the degree of structural control, the folded polymers are transformed into folded molecular brushes that are known to be visualizable as single molecule structures by AFM. The "grafting onto" approach is performed by using triazolinedione−diene reaction to graft the side chain polymers. A series of folded molecular brushes as well as the corresponding linear controls are synthesized. AFM visualization is proving the cyclization of the folded backbone by showing globular objects, where non-folded brushes show typical worm-like structures. © 2019 The Authors. *Journal of Polymer Science* published by Wiley Periodicals, Inc. J. Polym. Sci. **2020**, *58*, 154–162

KEYWORDS: atomic force microscopy (AFM); diselenide; grafted polymers; molecular bottle brushes; sequence-controlled polymers; single chain folding

INTRODUCTION The information rich biomacromolecules such as peptide/proteins, nucleotides/RNA/DNA, and saccharides have been source of inspiration for polymer sciences throughout decades.[1,2] Intense research was dedicated to mimic features of biopolymer classes with synthetic macromolecules.[3–5] However, designing polymers that can fold into structures with the precision, the complexity, and the variability of biomacromolecules is still demanding.[6–10]

The introduction of living/controlled polymerizations, including methods of controlled radical polymerization (CRP)[11] paved the way to access complex, multifunctional polymer architectures.[12–18] Routes to different topologies such as cyclic or multi-cyclic polymers were developed, by combining CRP with chain-end functionalization to induce intramolecular crosslinking.[19,20] More recently, block and statistical copolymers have been exploited to insert intramolecular bridges and thereby inducing single chain folding.[21–25] Covalent, dynamic covalent, and supramolecular bonds were used to generate static or dynamic single chain folding.[26–28] Elegant supramolecular single polymer chain compactions based on single or combination of orthogonal hydrogen-bonding tectons have been thoroughly reported.[29–31]

Although these synthetic approaches allowed the development of interesting 3D-structures, the crosslinks were often randomly distributed along the polymer chain, preventing the formation of discrete folds. The primary sequence is one of the key parameters in biomacromolecules to program precise interactions that enable access of specific functions including complex self-assembly.[4,32] With the onset of precision

---

Additional supporting information may be found in the online version of this article.

polymer chemistry, which aims at monodisperse macromolecules from fully synthetic monomer alphabets, polymers with discrete sequences get available.[33] Those promise both more controlled single chain folding mechanisms and access of complex 3D-structures. A rather broad range of synthesis strategies are available, including the use of templates,[34,35] solid-phase or solution iterative (sub)monomer synthesis,[36] multicomponent reactions,[37] CRP under single monomer insertion conditions,[38,39] and even molecular machines.[40] Some of these methods have already been investigated for the preparation of synthetic foldamers.[4,41] However, often only well-defined oligomers were provided and the synthesis of larger sequence-defined polymers remains challenging.[42] Sequence-regulated polymers became a promising detour on the way to next generation precision polymers and precision materials.[43] Controlled chain growth polymerizations combine both access to higher molecular weight polymers and functionality positioning. Sequence-regulated polymers can be accessed by ring opening metathesis polymerization, enabling to control the position of functional monomers along the polymer chain by exploiting substantially different growth rates of endo- and exo-norbornenes.[44] Initially sequence-regulated polymers were pioneered by positioning functional maleimide units along a styrene CRP.[45] This route took advantage of the low tendency of maleimides to homo-polymerize and the highly favored cross-propagation with styrene monomers. The styrene/maleimide copolymerization enabled the positioning of functional monomer units in growing polymer chains and controlled intramolecular crosslinking by click chemistry have been investigated.[46]

Polymers with dynamic intramolecular crosslinks have become relevant due to their ability to potentially reach equilibrium structures in response to environmental changes.[47] While dynamic bonds such as reversible cycloaddition and

disulfide bonds were intensively used to induce single chain organization,[48–50] diselenide bridges were less exploited. Xu et al. reported primarily the dynamic properties of diselenide linkages in synthetic polymers for controlled drug delivery applications,[51,52] or synthetic enzyme mimics.[53] Several methods were reported for the preparation of diselenide-containing polymers with various dynamic architectures[54,55] and displayed sensitivity to very soft external stimuli, including light, mild reducing or oxidizing agents. Generally, intramolecular crosslinking and single chain folding are analyzed by diffusion-ordered NMR spectroscopy or size exclusion chromatography (SEC), enabling to follow a distinct transition in hydrodynamic volume from the random linear polymer coil to a more compact folded coil structure. While coil compaction gets less prominent with increased molecular weight,[56] more complex structure folds demand to establish complementary analysis routes that enable to gain insights into structural features.

Herein, oxidative intramolecular crosslinking in fully synthetic sequence-controlled polymers was investigated, by using N-substituted maleimides bearing selenols to position diselenide bridges into a polystyrene backbone [Fig. 1]. Selenol oxidation in dilute conditions induces diselenide bridging and triggers single chain collapse. Besides proving cyclization by means of SEC and NMR, the folded polymers were transformed into grafted polymers and the resulting polymers enable conformation analysis by atomic force microscopy (AFM).

EXPERIMENTAL

The following chemicals were used as received. Blocbuilder MA (Arkema), hydrochloric acid 37% (VWR), 4-dimethylaminopyridine DMAP (Sigma-Aldrich), dithiobis(5-nitropyridine) (DTNP) (Sigma-Aldrich), 1,4 diazabicyclo[2.2.2]octane DABCO (Sigma-Aldrich), tris [2-(dimethylamino)ethyl] amine ME$_6$TREN (ABCR), N,N-diisopropyl ethylamine DIPEA (Sigma-Aldrich), N,N′-dicyclohexyl carbodiimide (DCC) (Sigma-Aldrich). N-Butyl acrylate (Sigma-Aldrich) was distilled at reduced pressure directly before use. 4-tert-Butoxystyrene S-OtBu (Sigma-Aldrich), anisole (Carl Roth), and dimethylformamide were passed through an alumina oxide column prior to use.

The synthesis of N-(2-para-methoxybenzyl selenoethyl) maleimide (Mal-SeMob) is described in the supporting information.

Sequence-Controlled Polymerization

Blocbuilder MA (1 equiv, 0.076 g) was dissolved in 2 mL of anisole and 3.8 mL of tertbutoxystyrene (100 equiv). The flask was deoxygenated by four freeze-pump-thaw cycles and filled with argon. The mixture was then immersed in a preheated bath at 120 °C. At time intervals, aliquots were taken from the mixture with a degassed syringe to monitor the monomer conversion by ^{1}H NMR. When the conversion reached approximately 10%, a degassed solution of Mal-SeMob (1.1 equiv, 0.071 g) in 0.2 mL of anisole was added to the polymerization. A second addition of degassed solution containing Mal-SeMob
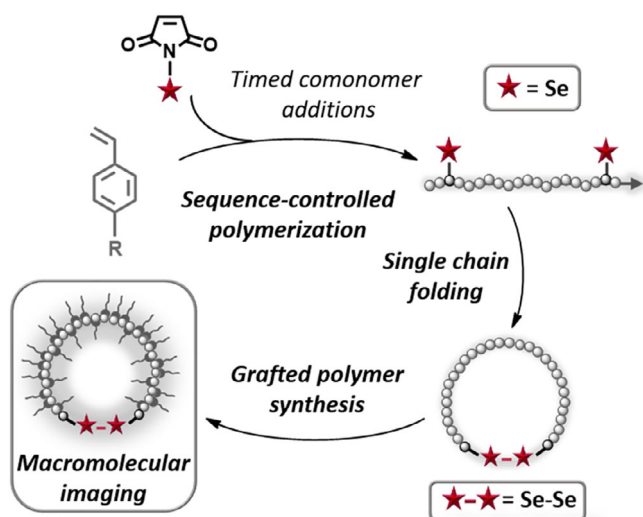

FIGURE 1 General synthetic strategy for controlled oxidative single chain folding and conformation visualization by AFM.

(1.1 equiv, 0.071 g) in 0.2 mL of anisole was performed when the conversion of tertbutoxystyrene reached 45%. The polymerization was stopped (50% of styrene conversion), and the polymer was precipitated in cold methanol (×3) and dried.

Removal of Tert-Butyl Group

The copolymer (M_n = 7,000 g/mol, 0.300 g) was dissolved in 70.0 mL of dioxane, and 1.5 mL of hydrochloric acid (37%) was added to the solution. The mixture was refluxed for 4.5 h at 105 °C. After completion of the hydrolysis, the polymer was precipitated in water and dried.

Intramolecular Diselenide Bridge Formation

2,2′-Dithiobis(5-nitropyridine) (7 equiv, 0.043 g) was dissolved in 600 mL of the solvent mixture methanol/TFA (80/20 v/v). The linear polymer precursor (1 equiv of selenol moieties, M_n = 7,000 g/mol, 0.070 g) was dissolved in 8 mL of methanol and was added dropwise to the flask via a syringe pump. The reaction was stirred for 4 days at room temperature. The solvent was removed under reduced pressure. The polymer was precipitated in water (×2) and in hexane (×1).

Ring Chain Opening by Oxidation

Three milligrams of cyclic polymers were dissolved in 1 mL of tetrahydrofuran, and 100 μL of hydrogen peroxide was added. The reaction was stirred overnight. The mixture was dried over $MgSO_4$ and concentrated under reduced pressure.

Synthesis of Cyclic Macroinitiator (c-PS-Diene$_{50}$)

The cyclic polymer (1 equiv of active centers, 0.015 g) was dissolved in 60 mL of dry acetonitrile under inert atmosphere and the solution was cooled in an ice bath. The symmetric anhydride of 2,4-hexadien-1-yl succinic acid monoester (5 equiv, 0.210 g) and 4-dimethylaminopyridine (5 equiv, 0.065 g) was added to the solution. The mixture was stirred at room temperature overnight. The solvent was removed under reduced pressure and the polymer was precipitated in methanol. The polymer was freeze-dried in benzene.

Synthesis of Urazole-Terminated Polymer (UR-PnBuA$_{40}$) and Oxidation (TAD-PnBuA$_{40}$)

Urazole-initiator (1.00 equiv, 0.060 g), n-butyl acrylate (45.00 equiv, 1.1 mL), Cu^0 (10 pellets), and 2.7 mL of DMF were degassed by four freeze-pump-thaw cycles and filled with inert gas. In a separate flask, ME_6TREN (0.15 equiv, 0.006 g), $CuBr_2$ (0.05 equiv, 0.001 g), and 3.0 mL of DMF were introduced and deoxygenated. The $CuBr_2$/ligand-solution was added to the reaction mixture. The reaction flask was then immersed in an oil bath at 25 °C. The polymerization was stopped at 75% of monomer conversion. The catalyst was removed by passing the reaction mixture over a column of Al_2O_3. The solvent and the monomer were removed under vacuum.

UR-PnBuA$_{40}$ (1 equiv of urazole group, 5,000 g/mol, 0.045 g) was dissolved in 2 mL of dry DCM. DABCO-Br (2 equiv, 0.029 g) was added to the solution and the mixture was stirred at room temperature for 3 h. After filtration, a red solution was obtained and TAD-PnBuA$_{40}$ was used without any further purification.

Synthesis of Grafted Polymers (GD = 65%)

c-PS-Diene$_{50}$ (1.0 equiv of active centers, 15,800 g/mol, 2.9 mg) was dissolved in 0.6 mL of dry DCM. A solution of TAD-PnBuA$_{40}$ polymer (1.0 equiv of TAD functionalities, 0.0450 g) in 2 mL of dry DCM was added dropwise to the reaction flask. The grafting reaction was stirred under inert atmosphere at room temperature for 14 h. The polymer was precipitated in methanol.

Synthesis of Molecular Brushes (GD = 100%)

c-PS-Diene$_{50}$ polymer backbone (1 equiv of active centers, 15,800 g/mol, 2.9 mg) was dissolved in 0.6 mL of dry DCM and was added dropwise to a solution of TAD-PnBuA$_{40}$ polymer (2 equiv of TAD functionalities, 0.0910 g) in 2 mL of dry DCM. The grafting reaction was stirred under inert atmosphere at room temperature for 14 h. The polymer was precipitated in cold methanol (×2).

RESULTS AND DISCUSSION

Sequence Controlled Polymerization

Controlled radical copolymerization of electron-rich styrene derivatives with a sub-stoichiometric amount of N-substituted maleimides allows the synthesis of copolymers with well-controlled molecular weight distribution and positioned insertions of maleimides along the polymer chain.[57] 4-tert-butoxystyrene (S-OtBu) was selected as styrene-based monomer, bearing a protected functionality that will later allow to introduce polymer side chains at each repeating unit to generate the molecular brush structure [Scheme 1 and Fig. 5]. This electron donor monomer enables strictly alternating
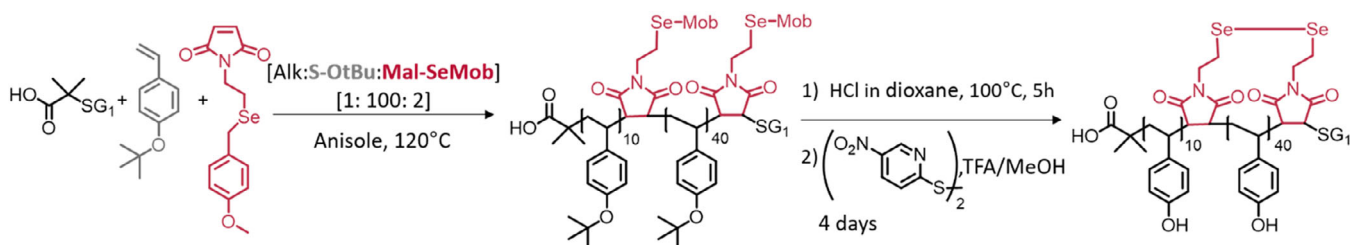
SCHEME 1 Synthetic route to polymers with positioned selenol entities for single chain folding by using NMP of 4-tert-butoxystyrene fed at suitable conversion with N-(2-para-methoxybenzyl selenoethyl) maleimide and subsequent folding by intramolecular diselenide bridge formation.

copolymerization with maleimides. An *N*-substituted maleimide containing a *para*-methoxybenzyl protected selenol moiety (Mal-SeMob) had to be synthesized as required acceptor monomer (Supporting Information). The Mal-SeMob synthesis was adapted from recent literature protocols.[58–60] Briefly, elemental selenium was reduced with hydrazine/sodium hydroxide to generate sodium diselenide, followed by reaction with *p*-methoxybenzyl chloride. Bis-(*p*-methoxybenzyl) diselenide was reduced to be reacted with 2-bromoethylamine. The *N*-substituted maleimide was obtained by reacting maleic anhydride with 2-(para-methoxy benzylseleno) ethylamine.

NMP of S-OtBu was initiated by using the alkoxyamine Blocbuilder MA to modulate the polymerization, and reaction kinetics were monitored by ^{1}H NMR spectroscopy [Fig. 2]. The NMP started with a homopolymerization up to ~10% conversion of S-OtBu after which 1 equiv of Mal-SeMob was added to the polymerization mixture. A second addition of 1 equiv of Mal-SeMob was provided at ~45% of S-OtBu conversion and the S-OtBu polymerization was allowed to reach ~50% before quenching.

The copolymerization kinetics demonstrated the full and precise incorporation of the functional maleimide units in narrow windows on both sides of the formed poly(S-OtBu) chains [Fig. 2(B)]. Indeed, for both additions, the conversion of

maleimides reached 100%. In average per addition, one Mal-SeMob unit was incorporated in each growing chain, while S-OtBu conversion increased by 7% only. Hence, both incorporation windows are narrowed down to seven S-OtBu units in average. The isolated sequence-controlled copolymer was analyzed by SEC and ^{1}H NMR spectroscopy. The proton spectrum confirmed the incorporation of the Mal-SeMob units in the growing polymer chains. Resonances corresponding to the Mob protective groups of the maleimide derivative were found at 7.17, 6.80, and 3.70 ppm [Fig. 2(A)]. Furthermore, the SEC analysis evidenced the formation of macromolecules with well-defined molecular weights and narrow dispersities [$M_{n,app}$ = 10,700, Đ = 1.11; Fig. 2(C)].

Backbone Deprotection

Removal of the *tert*-butyl protective group present at the poly (4-hydroxystyrene) backbone was achieved by HCl catalyzed hydrolysis and afford the linear deprotected precursor poly(*l*-PHS$_{50}$). Quantitative deprotection was confirmed by ^{1}H NMR, showing the absence of *tert*-butyl ether resonances at 1.0–1.5 ppm, while the resonances corresponding to the Mob-protected selenol were unaffected [Fig. S5].

Intramolecular Crosslinking

The formation of intramolecular diselenide bridges proceeded in a one-pot reaction that combines Mob-deprotection with selenol oxidation. To promote single chain collapse, the reaction was conducted under highly diluted conditions in a solvent mixture of methanol with 20 vol % trifluoroacetic acid. The reaction involved treatment with an excess of the electrophilic disulfide 2,2′-dithiobis(5-nitropyridine) (DTNP) under acidic conditions.[61] DTNP removed the 4-methoxybenzyl protecting group by substitution with a 2-thio-5-nitropyridine (S-Npys) group, leading to the protected selenol intermediate Se(S-Npys). The Se—S bond of the Se(S-Npys) is cleaved, generating free selenols that rapidly dimerized into diselenide groups by air oxidation.[62]

SEC, ^{1}H NMR, and 2D HSQC NMR characterized the cyclization process. As expected, the SEC traces of the linear and the

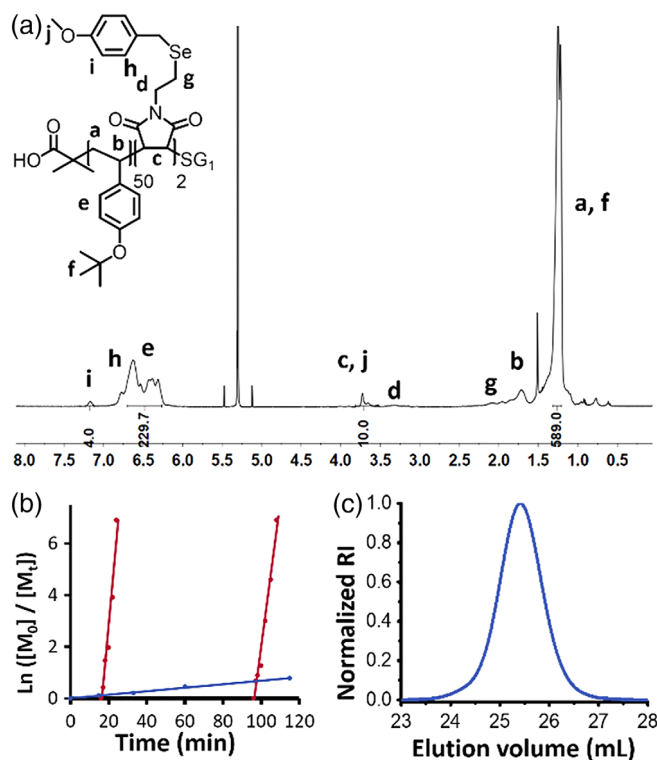**FIGURE 2** The prepolymer poly(S-OtBu) with positioned Mal-SeMob functionalities. ^{1}H NMR spectrum of the obtained copolymer (A). Semi logarithmic plot of monomer conversion versus time (B) and SEC curve of the copolymer (C).
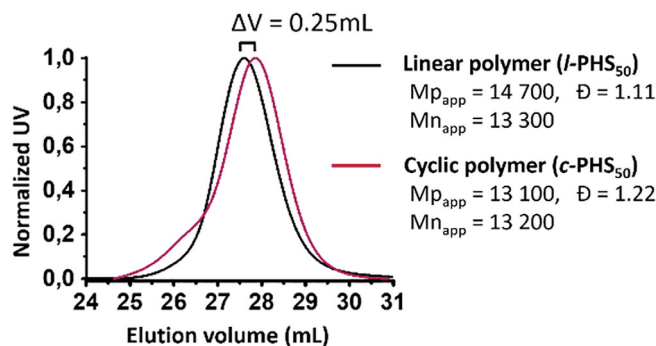

FIGURE 3 SEC traces of the linear precursor polymer poly(*l*-PHS$_{50}$) and the cyclic polymer poly(*c*-PHS$_{50}$) after deprotection/oxidation of selenols in highly diluted conditions.

folded polymers showed a shift toward lower apparent molecular weights [cf. Fig. 3; poly(l-PHS$_{50}$) vs. poly(c-PHS$_{50}$)] and confirmed the chain collapse by the reduction in hydrodynamic volume.[63] While the dispersity increased slightly to $Đ = 1.22$ the chromatograms showed a minor shoulder at the high-molecular-weight flank. This indicated that intramolecular oxidation dominated, and intermolecular oxidation occurred marginally to generate a small amount of chain dimerization. Proton NMR analysis indicated the absence of the characteristic resonances at 7.10, 6.80, and 3.70 ppm that correspond to the SeMob group and confirmed a complete deprotection of the selenol functionalities. 2D HSQC NMR spectroscopy provided evidence for diselenide bond formation [Fig. 4]. The spectra of the resulting cyclic polymers shows a clear shift of the resonance characteristic for the *CH$_2$*-Se

FIGURE 4 2D HSQC NMR spectra (MeOD-d$_4$) of the linear polymer poly(l-PHS$_{50}$) and the obtained cyclic polymer poly(c-PHS$_{50}$).

segment from 2.25/20.16 to 2.82/29.31 ppm. However, typical resonances of the intermediately protected selenols Se(S-Npys) were found with low intensities at 9.13, 8.32, and 7.82 ppm. The integral intensities indicated only 14% of selenol moieties to be still protected [Fig. S6]. It should be emphasized that the sequence-controlled polymerization and functionality positioning are limited in precision by the statistical radical growth process. It is expectable, that poly(S-OtBu) chains will be formed that contain for example, only one Mal-SeMob unit. Hence, a minor fraction will *per se* not be able to generate intramolecular diselenide bridges under full consumption of the intermediately protected selenols.

Ring Chain Opening

The redox sensitivity of diselenide bridge was exploited to confirm the cyclic topology. Oxidation of intramolecular diselenide moiety in the cyclic polymers leads to selenic acid and induces a reverse topology transition from cyclic to linear chains.[64] To prove this, the cyclic polymer was subjected to oxidation by using hydrogen peroxide, and the reaction was tracked by SEC. Indeed, after oxidation the polymer was shifted to lower elution time, which shows an increased hydrodynamic volume and confirmed indirectly the cyclization [Fig. S3].

Synthesis of Folded Brush Polymers for Macromolecular Imaging

To provide insight into the cyclization process at the molecular level the folded polymers were transformed into molecular brush structures to allow conformation analysis by AFM. While the "grafting from" procedure with atom transfer radical polymerization proved to be an effective access strategy to bottle brushes,[14,15] an interference of the CRP process with the diselenide bridges was evident (data not shown). Therefore, a "grafting onto" approach was chosen by exploiting triazolinedione (TAD) – diene cycloaddition reaction[65,66] to graft poly(n-butyl acrylate) (PnBuA) side chains onto the folded macromolecule backbone [Fig. 5(A)].[67]

A set of brush polymers with different grafting densities (GDs) was synthesized to investigate the visualization of folded polymer chains. The cyclic polymer c-PHS$_{50}$ was taken as precursor polymer to constitute the backbone. c-PHS$_{50}$ had a DP$_n$ of 50 *para*-hydroxystyrene repeats and in average between the locations DP ≈ 10 and DP ≈ 40 the diselenide bridge. The conjugated diene fragment that is necessary for the TAD–diene cycloaddition was introduced to c-PHS$_{50}$ by esterification of the hydroxyl functionalities with the symmetric anhydride of 2,4-hexadien-1-yl succinic acid monoester to yield c-PS-Diene$_{50}$. The ^{1}H-NMR spectrum proved the quantitative reaction by the appearance of a series of resonances from 5.61 to 6.24 ppm that were assigned to the diene structure [Fig. S7]. SEC suggested a clean polymer modification reaction, where the dispersity remained unchanged, $Đ = 1.22$. Moreover, a shift of the SEC trace to higher apparent molecular weights was evident if the deprotected phenolic precursor polymer c-PHS$_{50}$ was compared to the product c-PS-Diene$_{50}$ with $M_{n,app} = 14,400$ [Fig. 5(B), traces of c-PS-Diene$_{50}$]. The TAD-terminated PnBuA was synthesized according to the literature by Cu^0-mediated polymerization,
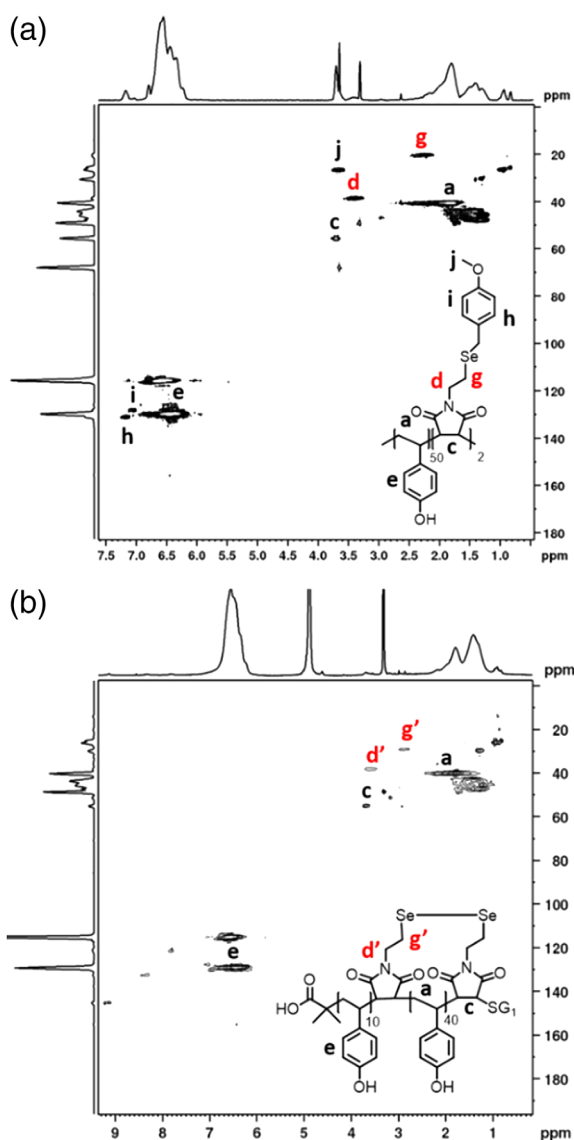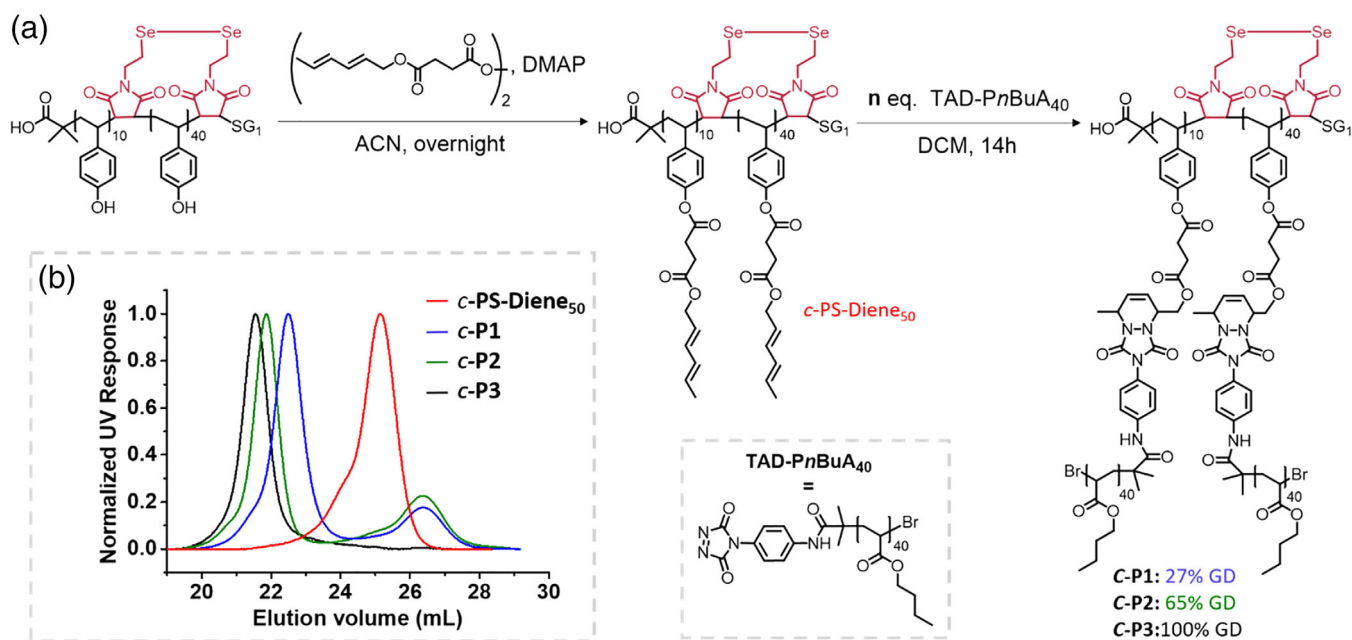
FIGURE 5 (A) Synthetic of molecular brush polymers by applying the "grafting onto" strategy (A) and respective SEC analysis of functionalized cyclic precursor polymer (c-PS-Diene$_{50}$) and the set of bottle brush polymers exhibiting different GD of PnBuA$_{40}$ side chains (B) (c-P1, c-P2 crude samples, c-P3 purified).

using an urazole-containing initiator.[65] Urazole-terminated PnBuA with DP$_{n,NMR}$ = 40 was prepared (UR-PnBuA$_{40}$; Đ = 1.20). The UR-PnBuA$_{40}$ could be quantitatively activated by the reaction with bis-bromine-1,4-diazabicyclo [2.2.2]octane (DABCO-Br) complex to afford TAD-PnBuA$_{40}$. The folded molecular brushes were synthesized by TAD-diene cycloaddition, reacting the cyclic precursor polymer c-PS-Diene$_{50}$ with defined quota of TAD-PnBuA$_{40}$. The side chain GD on the backbone could be adjusted with the molar ratio of diene to TAD (Table 1). While a ratio of 0.7/1 (TAD/diene groups of c-PS-Diene$_{50}$) resulted in only 27% GD of side chains on the cyclic backbone (c-P1), an ratio of 1/1 resulted in 65% GD (c-P2) and an excess of 2/1 was necessary to push the GD to 100% (c-P3). ^{1}H NMR spectroscopy confirmed the intensity decrease of the diene resonances and the appearance of new resonances at 5.87 and 5.78 ppm related to the formed alkenes [Fig. S9-11]. The cycloaddition proved with low molecular species to proceed fast, reaching quantitative conversion under stoichiometric conditions. As expected, the steric load and the osmotic pressure of a polymer-to-polymer

grafting reaction reduced both ligation rates and achievable conversions.

Figure 5(B) provides the SEC traces of the crude grafted polymers, showing a clear and clean shift from the c-PS-Diene$_{50}$ precursor to the brushes c-P1, c-P2, and c-P3 on GD 27%, 65%, and 100%, respectively. The SEC traces of the brushes appeared with monomodal peak shapes and the low dispersity values of Đ < 1.10 confirmed the good control during synthesis of the backbone precursor polymer and the grafting process. As a control sample, a linear brush analogue was synthesized by using a similar non-folded polymer precursor poly (l-PHS$_{50}$) to generate l-PS-Diene$_{50}$ to which TAD-PnBuA$_{40}$ were grafted with a medium GD of 43%, giving the linear, not folded molecular brush analogue l-P2.

While grafting conditions for both brushes c-P2 and l-P2 have been identical, and a moderate GD was achieved for both products, a divergence of GDs was evident (65% GD for the cyclic vs. 43% GD for the linear analogue). The grafting onto

TABLE 1 Reaction Conditions of Molecular Brush Polymers Synthesis and Characterization

	Grafting onto: molar ratio TAD/diene[a]	GD$_{NMR}$[b] (%)	$M_{n,NMR}$[c] (g/mol)	$M_{n,SEC}$[d] (g/mol)	Đ$_{brush,SEC}$[e]
c-P1	0.70/1	27	86,000	58,000	1.08
c-P2	1.0/1	65	182,000	78,000	1.06
c-P3	2.0/1	100	280,000	89,000	1.03

[a] Coupling reaction of c-PS-Diene$_{50}$ with TAD-PnBuA$_{40}$ in DCM for 14 h at RT.
[b] ^{1}H-NMR in CDCl$_3$. GD$_{NMR}$ calculated by using the equation GD$_{NMR}$ = (1 − [Diene]$_t$/[Diene]$_{initial}$) × 100.
[c] Calculated from ^{1}H NMR by using the equation $M_{n,NMR}$ = M$_n$ (c-PS-Diene$_{50}$) + GD$_{NMR}$ × DP$_{Backbone}$ × M$_n$ (PnBuA$_{40}$).
[d] Determined by SEC in THF, based on PS calibration.
[e] Grafting density calculated from $M_{n,SEC}$.

approach is certainly not the most straightforward method to achieve bottlebrush polymers, as the grafting process is sensitive to various parameters such as local GD, accessibility of functionalities to be grafted onto, local osmotic pressure, and steric shielding in the brushes. The different GDs might indicate some effects of backbone topology on the reachable conversion. Obviously, the cyclic polymer backbone precursor was more prone to effective grafting, compared to the linear analogue. Potentially, this might be rationalized by a reduced degree of freedom of the backbone segment conformation found in the cyclic polymer precursor, compared to the more flexible segments in the linear precursor, which could influence the diffusion of free side chains.

Atomic Force Microscopy

AFM characterization was used to investigate the possibility to distinguish differences between cyclic and linear brush topologies and access the degree of structural control at the molecular level [Fig. 6(A)]. Taking advantage of both the lateral pressure arising from the high GD of the side chains that drives the brush backbone to adopt an extended chain structure and the strong interactions of PnBuA with mica substrates, the visualization of those bottle brush molecules should be feasible.[15,68–70]

All samples were prepared in a standardized manner by spin coating from a dilute polymer solution onto mica substrates. Already the crude cyclic brush polymers c-P2 showed mainly globular structures with non-corrected diameters in the range of 20–30 nm [Fig. 6(B) and Fig. S14]. In addition, some indications of a typical PnBuA corona structure are evident that would meet expectations of a collapsed brush topology with side chains spread-out on the substrate surface. However, the structure dimensions and topologies will be certainly influenced by the significant amount of TAD-PnBu$_{40}$ free side chains, which decreases the achievable image resolution and probably swell the primary brush structures. In the crude mixture of all grafting onto reactions, a significant amount of unreacted TAD-PnBuA$_{40}$ could be found not attached to the backbone polymer [Fig. 5(B); traces c-P1 and c-P2]. In order to allow the visualization of the molecular brush polymers by means of AFM, the crude brush polymers had to be purified by SEC chromatography in order to remove excess of the unreacted side chains. High-molecular-weight peaks that correspond to the molecular brushes were collected from a standard analytical SEC setup. While single runs were only required to purify c-P2 and l-P2, multiple runs were necessary to isolate sufficient amounts of c-P3.

The purified c-P2 could be visualized more clearly by AFM [Fig. 6(C) and Fig. S15]. Interestingly, the topology of the nano-objects remained globular, as indicated by the fried egg-like structure observable. The objects shown in the phase images had height of ~0.8 nm and an average, non-tip corrected diameter in the range of 26 nm. The cross section profiles in two perpendicular scan directions revealed practically identical height profiles and confirmed the isometric structure with uncorrected full width at half maximum
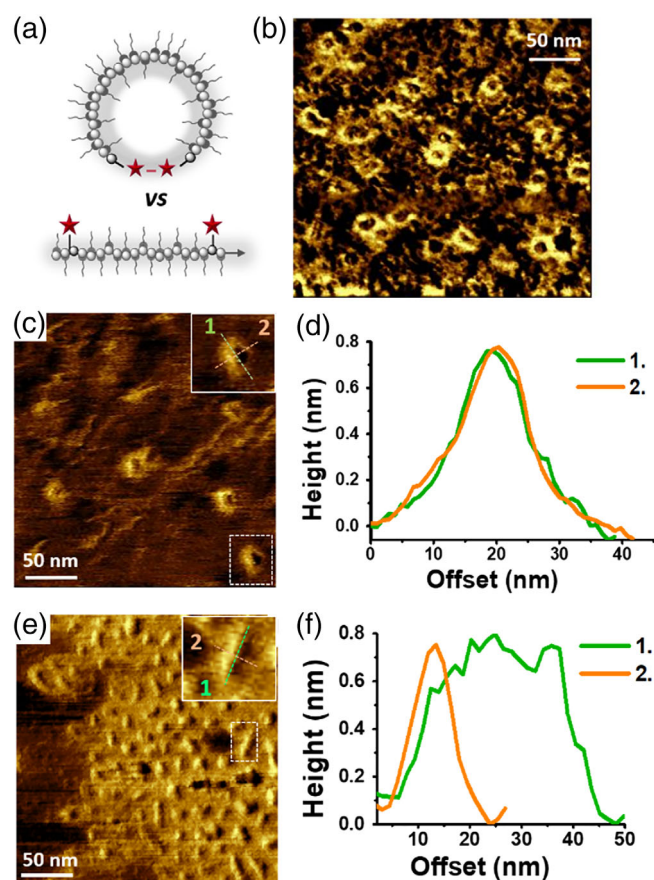

FIGURE 6 Schematic illustration of cyclic versus linear bottle brushes (A). AFM micrographs of crude c-P2 polymer with large fraction of free TAD-PnBuA$_{40}$ (B), purified c-P2 (C), and purified linear analogue l-P2 (E). Cross-section profiles of representative structures from C&E are provided in D&F (conditions: spin coating from CHCl$_3$ solution of 0.01 mg/mL brush concentration, freshly cleaved mica, phase image).

(FWHM) in the range of about 18 nm [Fig. 6(D)]. Generally, molecular brush polymers with sufficiently long PnBuA$_{40}$ side chains have a high tendency to adapt extended worm-like structures.[14] The observation of globular objects could potentially suggest the presence of a folded backbone structure, where the full extension of the brush backbone is prevented due to intramolecular diselenide bridges that lock the backbone into a cyclic topology. For comparison, the AFM micrographs of the linear polymer brush analogue (l-P2) were investigated. As expected, the non-cyclic brush polymers exhibit worm-like structures [Fig. 6(E) and Fig. S16]. The micrograph showed a rather obvious polydispersity in length. This reflects on the one hand the dispersity of the backbone polymer poly(l-PHS$_{50}$), but could on the other hand potentially be caused by partial backbone collapse due to inhomogeniuous grafting density along the backbone.[15] The cross-section profiles obtained along two perpendicular scan lines confirmed the aniometry of worm-like objects [Fig. 6(F)]. The average structure width of 22 nm could be rather

precisely determined by measuring height maximum distances of molecular brushes in dense structure packages. As expected, this dimension is in the similar range as the object width found before in the c-P2 structures. The linear brush structures reach lengths of about 27 nm. If a monomer repeating unit length of 0.24 nm is considered, this could be explained by a fully extended poly(styrene)$_{50}$ backbone spanning 12 nm (50×0.24 nm) and two times a corona of PnBuA$_{40}$ side chains, stretching maximum contour length of 9.6 nm in all directions (40×0.24 nm). Despite the fact, that the image and statistics are not optimal, also the dimensions of the globular objects from the cyclic c-P2 are in the range of an expected theoretical structure. Considering that in an idealized cyclic brush structure, the c-PS-Diene$_{50}$ backbone spans a length of 12 nm, that is, the circumference of a cycle with a diameter of 3.8 nm ($c = \pi \times d$). To this backbone, the 9.6 nm corona of PnBuA$_{40}$ side chains can be added that stretch-out in all directions. This idealized donut-shape is unlikely to be adapted, would however, have an expected diameter of 22.8 nm. Considering that the brush has only 65% GD, the PnBuA$_{40}$ side chains will not be fully all-trans extended, which would explain the experimentally observed size of FWHM ~18 nm.

CONCLUSIONS

The sequence-controlled styrene/maleimide CRP platform was utilized to design polymers containing protected selenol fragments at precisely defined positions in the polymer chain. Diselenide dynamic covalent bond was exploited to generate intramolecular crosslinking and the cyclization process was successfully characterized. A simple strategy for visualizing single chain conformation by AFM was developed. The folded polymers were transformed into molecular brush polymers that could be analyzed by AFM. Macromolecules exhibiting globular fried egg-like shape structures were successfully visualized, where the dimensions meet the range of the expected idealized structure. The non-folded controls show the typical worm-like structures of molecular bottlebrushes. This analytic tool allowed direct visualization of single chain folding and therefore gaining insights into the degree of structural control. This synthetic strategy could give access to an additional analytic tool for characterizing more complex synthetic macromolecule folding.

REFERENCES AND NOTES

1 C. T. J. Branden, *Introduction to Protein Structure*; Garland Publishing: New York, **1998**.

2 J.-F. Lutz, M. Ouchi, D. R. Liu, M. Sawamoto, *Science* **2013**, *341*, 1238149.

3 J.-F. Lutz, H. G. Börner, *Macromol. Rapid Commun.* **2011**, *32*, 113.

4 N. Badi, J.-F. Lutz, *Chem. Soc. Rev.* **2009**, *38*, 3383.

5 M. Ouchi, N. Badi, J.-F. Lutz, M. Sawamoto, *Nat. Chem.* **2011**, *3*, 917.

6 D. A. Tomalia, A. M. Naylor, W. A. Goddard, *Angew. Chem. Int. Ed.* **1990**, *29*, 138.

7 S. Hecht, J. M. J. Fréchet, *Angew. Chem. Int. Ed.* **2001**, *40*, 74.

8 I. Huc, *Eur. J. Org. Chem.* **2004**, *2004*, 17.

9 D. W. Zhang, X. Zhao, J. L. Hou, Z. T. Li, *Chem. Rev.* **2012**, *112*, 5271.

10 B. Voit, *J. Polym. Sci. Part A: Polym. Chem.* **2005**, *43*, 2679.

11 W. A. Braunecker, K. Matyjaszewski, *Prog. Polym. Sci.* **2007**, *32*, 93.

12 K. A. Davis, K. Matyjaszewski, *Statistical, Gradient, Block and Graft Copolymers by Controlled/Living Radical Polymerizations*. Advances in Polymer Science; Springer: Berlin, Heidelberg, **2002**.

13 S. Qin, K. Matyjaszewski, *Macromolecules* **2003**, *36*, 605.

14 K. L. Beers, S. G. Gaynor, K. Matyjaszweski, *Macromolecules* **1998**, *31*, 9413.

15 H. G. Börner, D. Duran, K. Matyjaszewski, M. Da Silva, S. S. Sheiko, *Macromolecules* **2002**, *35*, 3387.

16 F. S. Bates, M. A. Hillmyer, T. P. Lodge, C. M. Bates, K. T. Delaney, G. H. Fredrickson, *Science* **2012**, *336*, 434.

17 N. Hadjichristidis, M. Pitsikalis, S. Pispas, H. Iatrou, *Chem. Rev.* **2001**, *101*, 3747.

18 K. Matyjaszewski, J. Spanswick, *Mater. Today* **2005**, *8*, 26.

19 M. R. Whittaker, Y. K. Goh, H. Gemici, T. M. Legge, S. Perrier, M. J. Monteiro, *Macromolecules* **2006**, *39*, 9028.

20 B. A. Laurent, S. M. Grayson, *Chem. Soc. Rev.* **2009**, *38*, 2202.

21 E. Harth, B. Van Horn, V. Y. Lee, D. S. Germack, C. P. Gonzales, R. D. Miller, C. J. Hawker, *J. Am. Chem. Soc.* **2002**, *124*, 8653.

22 O. Altintas, C. Barner-Kowollik, *Macromol. Rapid Commun.* **2015**, *37*, 29.

23 T. Terashima, T. Sugita, K. Fukae, M. Sawamoto, *Macromolecules* **2014**, *47*, 589.

24 M. Seo, B. J. Beck, J. M. J. Paulusse, C. J. Hawker, S. Y. Kim, *Macromolecules* **2008**, *41*, 6413.

25 B. S. Murray, D. A. Fulton, *Macromolecules* **2011**, *44*, 7242.

26 C. Heiler, J. T. Offenloch, E. Blasco, C. Barner-Kowollik, *ACS Macro Lett.* **2016**, *6*, 56.

27 S. Mavila, O. Eivgi, I. Berkovich, N. G. Lemcoff, *Chem. Rev.* **2016**, *116*, 878.

28 T. S. Fischer, D. Schulze-Sunninghausen, B. Luy, O. Altintas, C. Barner-Kowollik, *Angew. Chem. Int. Ed.* **2016**, *55*, 11276.

29 N. Hosono, M. A. Gillissen, Y. Li, S. S. Sheiko, A. R. Palmans, E. W. Meijer, *J. Am. Chem. Soc.* **2013**, *135*, 501.

30 T. Mes, R. van der Weegen, A. R. Palmans, E. W. Meijer, *Angew. Chem. Int. Ed.* **2011**, *50*, 5085.

31 G. M. t. Huurne, A. R. A. Palmans, E. W. Meijer, *CCS Chem.* **2019**, *1*, 64.

32 J.-F. Lutz, *Polym. Chem.* **2010**, *1*, 55.

33 J.-F. Lutz, *Macromol. Rapid Commun.* **2017**, *38*, 1700582.

34 S. Mochizuki, N. Ogiwara, M. Takayanagi, M. Nagaoka, S. Kitagawa, T. Uemura, *Nat. Commun.* **2018**, *9*, 329.

35 N. ten Brummelhuis, *Polym. Chem.* **2015**, *6*, 654.

36 R. B. Merrifield, *J. Am. Chem. Soc.* **1963**, *85*, 2149.

37 S. C. Solleder, M. A. R. Meier, *Angew. Chem. Int. Ed.* **2014**, *53*, 711.

38 J. Vandenbergh, G. Reekmans, P. Adriaensens, T. Junkers, *Chem. Commun.* **2013**, *49*, 10358.

39 J. De Neve, J. J. Haven, L. Maes, T. Junkers, *Polym. Chem.* **2018**, *9*, 4692.

40 B. Lewandowski, G. De Bo, J. W. Ward, M. Papmeyer, S. Kuschel, M. J. Aldegunde, P. M. E. Gramlich, D. Heckmann, S. M. Goldup, D. M. D'Souza, A. E. Fernandes, D. A. Leigh, *Science* **2013**, *339*, 189.

41 T. B. Yu, J. Z. Bai, Z. Guan, *Angew. Chem. Int. Ed.* **2009**, *48*, 1097.

42 J.-F. Lutz, *Sequence-Controlled Polymers*; Wiley-VCH: Weinheim, **2018**.

43 J.-F. Lutz, J.-M. Lehn, E. W. Meijer, K. Matyjaszewski, *Nat. Rev. Mater.* **2016**, *1*, 16024.

44 D. Moatsou, C. F. Hansell, R. K. O'Reilly, *Chem. Sci.* **2014**, *5*, 2246.

45 S. Pfeifer, J.-F. Lutz, *J. Am. Chem. Soc.* **2007**, *129*, 9542.

46 B. V. Schmidt, N. Fechler, J. Falkenhagen, J.-F. Lutz, *Nat. Chem.* **2011**, *3*, 234.

47 A. Sanchez-Sanchez, J. A. Pomposo, *Part. Part. Syst. Charact.* **2014**, *31*, 11.

48 B. T. Tuten, D. Chao, C. K. Lyon, E. B. Berda, *Polym. Chem.* **2012**, *3*, 3068.

49 O. Shishkan, M. Zamfir, M. A. Gauthier, H. G. Börner, J.-F. Lutz, *Chem. Commun.* **2014**, *50*, 1570.

50 O. Altintas, C. Barner-Kowollik, *Macromol. Rapid Commun.* **2012**, *33*, 958.

51 W. Lu, X. Pan, Z. Zhang, J. Zhu, N. Zhou, X. Zhu, *Polym. Chem.* **2017**, *8*, 3874.

52 N. Ma, Y. Li, H. Xu, Z. Wang, X. Zhang, *J. Am. Chem. Soc.* **2010**, *132*, 442.

53 H. Xu, W. Cao, X. Zhang, *Acc. Chem. Res.* **2013**, *46*, 1647.

54 X. Pan, F. Driessen, X. Zhu, F. E. Du Prez, *ACS Macro Lett.* **2017**, *6*, 89.

55 M. M. Stamenović, P. Espeel, E. Baba, T. Yamamoto, Y. Tezuka, F. E. Du Prez, *Polym. Chem.* **2013**, *4*, 184.

56 D. Cho, K. Masuoka, K. Koguchi, T. Asari, D. Kawaguchi, A. Takano, Y. Matsushita, *Polym. J.* **2005**, *37*, 506.

57 S. Srichan, D. Chan-Seng, J.-F. Lutz, *ACS Macro Lett.* **2012**, *1*, 589.

58 D. Plano, Y. Baquedano, D. Moreno-Mateos, M. Font, A. Jimenez-Ruiz, J. A. Palop, C. Sanmartin, *Eur. J. Med. Chem.* **2011**, *46*, 3315.

59 B. J. Bhuyan, G. Mugesh, *Org. Biomol. Chem.* **2011**, *9*, 1356.

60 N. Matuszak, G. G. Muccioli, G. Labar, D. M. Lambert, *J. Med. Chem.* **2009**, *52*, 7410.

61 K. M. Harris, S. Flemer, R. J. Hondal, *J. Pept. Sci.* **2007**, *13*, 81.

62 A. L. Schroll, R. J. Hondal, S. Flemer, *J. Pept. Sci.* **2012**, *18*, 155.

63 H. R. Kricheldorf, *J. Polym. Sci. Part A: Polym. Chem.* **2010**, *48*, 251.

64 C. Wang, X. An, M. Pang, Z. Zhang, X. Zhu, J. Zhu, F. E. Du Prez, X. Pan, *Polym. Chem.* **2018**, *9*, 4044.

65 S. Billiet, K. De Bruycker, F. Driessen, H. Goossens, V. Van Speybroeck, J. M. Winne, F. E. Du Prez, *Nat. Chem.* **2014**, *6*, 815.

66 K. De Bruycker, S. Billiet, H. A. Houck, S. Chattopadhyay, J. M. Winne, F. E. Du Prez, *Chem. Rev.* **2016**, *116*, 3919.

67 L. Xiao, Y. Chen, K. Zhang, *Macromolecules* **2016**, *49*, 4452.

68 H. G. Börner, K. Beers, K. Matyjaszewski, S. S. Sheiko, M. Möller, *Macromolecules* **2001**, *34*, 4375.

69 M. O. Gallyamov, B. Tartsch, P. Mela, I. I. Potemkin, S. S. Sheiko, H. G. Börner, K. Matyjaszewski, A. R. Khokhlov, M. Möller, *J. Polym. Sci. Part B: Polym. Phys.* **2007**, *45*, 2368.

70 S. S. Sheiko, M. Möller, *Chem. Rev.* **2001**, *101*, 4099.